

# High-Resolution Nuclear Magnetic Resonance of Solids

Gary E. Maciel

Nuclear magnetic resonance (NMR) has during the past 30 years emerged as one of the most powerful approaches for elucidation of structure and dynamics in pure and applied chemistry (1). It has achieved almost unparalleled popularity for providing details of molecular structure and dynamics in chemistry and areas of research and development related to chemistry. This popularity is largely

ability to distinguish resonances with reasonably different chemical shifts.

A major technical goal of NMR has been to develop techniques for narrowing the resonance lines without sacrificing too much information on chemical structure or dynamics in the process. This task has been typically much more difficult for solid samples than for liquids, and this is why high-resolution

---

*Summary.* The development of line-narrowing techniques, such as magic-angle spinning (MAS) and high-power decoupling, has led to powerful high-resolution nuclear magnetic resonance approaches for solid samples. In favorable cases (for instance, where high abundances of protons are present) cross polarization (CP) provides a means of circumventing the time bottleneck caused by inefficient spin-lattice relaxation in many solids. The combined CP-MAS approach for carbon-13 with proton decoupling has become a popular and routine experiment for organic solids. For many nuclides with spin quantum number  $I > 1/2$  the central nuclear magnetic resonance transition can be employed in high-resolution experiments that involve rapid sample spinning. A continuing stream of advances holds great promise for the use of high-resolution techniques for the characterization of solids by a wide range of nuclides.

---

based on the high-resolution character of most NMR experiments. For present purposes, we can define a "high-resolution" spectrum as one in which individual details of molecular structure are manifested in specific regions or by specific patterns in the spectrum, which are distinguishable within the available characteristics of spectral dispersion and line widths. In NMR studies of liquid samples, this typically means that the dispersion of chemical shifts and the magnitudes of pertinent, indirect ( $J$ ) spin-spin coupling constants are considerably larger than the natural widths of the resonances; otherwise overlaps will preclude distinguishing between the individual resonance lines on which structural interpretations of the spectra depend. For solid samples, the line widths that are normally attainable with available techniques usually obscure the small  $J$  couplings that are often so useful in liquid-state NMR; hence, the usual criterion for high resolution in solid samples is the

NMR has been essentially a liquid-state technique until recently, and why analysis of liquid samples remains by far the most common type of NMR application.

There are two main reasons why high-resolution NMR has so far been largely limited to liquid samples. These are the severe line-broadening effects characteristic of the NMR of immobile or solid-state systems (together with the associated sensitivity problem in spreading a given signal intensity over a broad line) and the inherent sensitivity problems of NMR (associated with the relatively low measuring frequencies employed in NMR). This last difficulty has been alleviated by a steady succession of improvements in NMR instrumentation (for instance, higher magnetic fields). The line-broadening problems have been addressed successfully by the continuing development of line-narrowing techniques for the NMR of solids (2), as described below.

Line-broadening effects are more diffi-

cult problems in solid-state NMR than for liquid samples because the rapid, random motions characteristic of liquids bring about a natural averaging of line-broadening influences. In order to obtain sharp NMR lines for solids, where the motions are more constrained, this kind of averaging must be brought about artificially by specific line-narrowing techniques, and these techniques constitute the basis of modern high-resolution NMR approaches for solid samples (3).

In spite of the relative ease of obtaining high-resolution NMR spectra of liquid samples and the relative difficulty of employing line-narrowing techniques for solids, there are more often compelling reasons for carrying out NMR experiments on solid samples. Of course, in some cases it is simply not possible to dissolve a solid sample of interest under conditions such that the structural integrity of the sample is retained; examples are heterogeneous catalysts and coal. In other cases it may be possible to dissolve a solid sample, so that liquid-state experiments can be carried out, but it may be the properties of the solid that are primarily of interest; one expects this to be the case frequently with synthetic polymers. Also, the availability of high-resolution NMR techniques for solids permits the use of NMR as a structure-determination bridge between the solid and liquid states of matter. This can prove useful in analytical work, where it is often pertinent to examine both a solid residue and an extract in an analytical procedure, and it is highly relevant in fundamental structural chemistry. The most common source of detailed, accurate information on chemical structure is x-ray diffraction data on crystalline solids; yet chemical reactivity (and hence structure) is usually of more interest in the liquid-solution state. High-resolution NMR now has the capability of bridging this gap, in a sense extrapolating into the liquid state information that has been determined on crystals by x-ray diffraction.

This article is concerned with recent developments in techniques for obtaining high-resolution NMR spectra on solid samples and with a perspective on the kinds of applications for which these techniques are well suited. Carbon-13 is used as the example for much of this article, but other important examples are also addressed, and much of what is presented in terms of  $^{13}\text{C}$  is largely transferable to a variety of other nuclides.

---

Gary E. Maciel is a professor in the Department of Chemistry, Colorado State University, Fort Collins 80523.

## Characteristics of NMR of Solids:

### Powder Patterns and Line Narrowing

In high-resolution approaches, the main NMR parameter that is usually of interest in applications is the "isotropic" chemical shift—the parameter that is commonly measured for liquid samples. However, for highly immobile species, such as those in rigid solids or in adsorbates tightly attached to a rigid solid surface, a straightforward experiment of the type routinely carried out with modern equipment to display isotropic chemical shift differences for liquid samples gives a very disappointing, almost featureless spectrum. Such spectra manifest not only the dependence of the isotropic chemical shift on the local chemical environment, but also the dependence of the chemical shift on the geometric relationship between that local environment and the direction of the static magnetic field,  $H_0$  (2). This second factor is referred to as the chemical shift anisotropy (CSA). The net result of the CSA is that, for a static amorphous or powdered crystalline sample, the entire range of chemical shifts spanned by all possible orientations is present in the spectrum. The result is known as a CSA powder pattern and is seen schematically in Fig. 1a for the case of the  $^{13}\text{C}$  resonance of a very simple system (such as frozen formaldehyde, with proton decoupling) that is in a powdered form or an amorphous state or is tightly adsorbed in some specific manner on the surface of a pow-

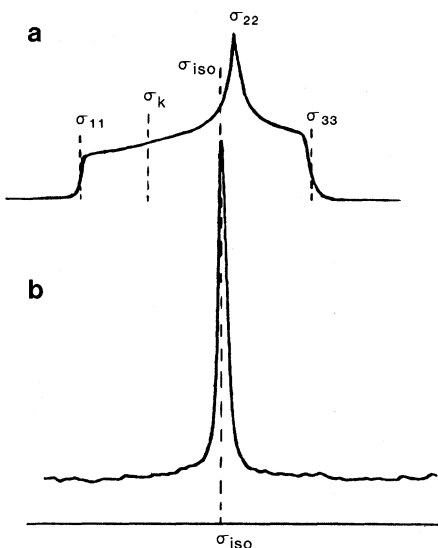


Fig. 1. (a) Chemical shift anisotropy powder pattern for a single type of carbon, showing the principal elements of the chemical shift tensor ( $\sigma_{11}$ ,  $\sigma_{22}$ ,  $\sigma_{33}$ ) and the chemical shift ( $\sigma_k$ ) for one particular orientation of the molecule. (b) Result of magic-angle spinning, giving the isotropic chemical shift ( $\sigma_{\text{iso}}$ ).

dered or amorphous material. This pattern displays the three principal elements of the shielding tensor ( $\sigma_{11}$ ,  $\sigma_{22}$ ,  $\sigma_{33}$ ) rather than just the isotropic average  $\sigma_{\text{iso}} = (1/3)(\sigma_{11} + \sigma_{22} + \sigma_{33})$  that one would observe for a liquid sample.

As attractive as it may seem to have three chemical shift parameters ( $\sigma_{11}$ ,  $\sigma_{22}$ ,  $\sigma_{33}$ ) rather than only the one ( $\sigma_{\text{iso}}$ ) obtained for liquids, the fact that the breadth of the CSA pattern for  $sp$  or  $sp^2$  carbon is typically 100 to 200 ppm (up to about 50 ppm for  $sp^3$  carbons) means that severe overlaps occur between the CSA powder patterns of systems with an appreciable degree of structural complexity. Hence, for most practical applications, a CSA line-narrowing technique is needed. For liquids this line narrowing is provided by nature in the form of rapid, random motional averaging. For rigid systems averaging of the CSA is accomplished mechanically by rapid spinning of the sample about an axis making an angle of  $54^\circ 44'$  ( $\cos^{-1} \sqrt{1/3}$ ) with  $H_0$  (4). The result is shown in Fig. 1b, and the technique is referred to as magic-angle spinning (MAS).

Magic-angle spinning can in principle, and sometimes in practice, also be used to eliminate another important line-broadening interaction, the magnetic dipole-dipole interaction between pairs of nuclear magnetic moments. This interaction is depicted for a  $^{13}\text{C}$ - $^1\text{H}$  pair in Fig. 2, together with the classical expression for the energy of this interaction and the effect of rapid sample spinning on the interaction. It is readily seen that the dipole-dipole interaction can be averaged to zero if MAS is applied. However, in order to accomplish this averaging straightforwardly it is necessary to spin the sample at a speed that is large compared to the size of the dipole-dipole line-broadening effect.

Because of the large size of the nuclear magnetic moment of a proton and the generally high abundance of protons in many samples, on the average each proton magnetic moment experiences strong torques exerted by one or more other proton magnetic moments. The net result is spin-spin "flip-flops" (5) in which two protons simultaneously interchange spin states, as depicted in Fig. 3; the associated energy exchange between the spins is facilitated by the fact that both spins are protons, and hence have the same Larmor frequencies and Zeeman energy levels (so the energy loss for one proton is compensated by the energy gain of the other). Because of the effects of these strong  $^1\text{H}$ - $^1\text{H}$  dipolar interactions, it is usually not possible to average

$^1\text{H}$ - $^1\text{H}$  dipolar interactions by MAS. For related reasons it is often not possible to handle dipolar interactions of protons with other nuclides efficiently by MAS. However, for the observation of nuclei other than protons, high-power  $^1\text{H}$  decoupling can be used to eliminate the line-broadening effects of dipolar interactions with protons (6). This is completely analogous to the low-power  $^1\text{H}$  decoupling used routinely in liquid-sample NMR to remove effects of indirect ( $J$ ) coupling between  $^{13}\text{C}$  and  $^1\text{H}$ . The process can be viewed as stimulating rapid transitions (inversions) of  $^1\text{H}$  spin states, so that the average  $^1\text{H}$  dipolar effect on  $^{13}\text{C}$  vanishes.

Elimination of homonuclear dipolar broadening in solid-state NMR spectroscopy has been a major challenge in NMR research. Clearly, it is not possible simply to use high-power decoupling if one is trying to observe the same nuclei that one is trying to decouple. An approach that has shown considerable promise is the use of sophisticated multiple-pulse sequences, in which the proton spins are manipulated to give a zero average of the  $^1\text{H}$ - $^1\text{H}$  dipolar interactions (7), rather than relying on motional averaging of the trigonometric factor representing the orientation dependence of the type shown in Fig. 2. This multiple-pulse approach requires the generation of short, intense,

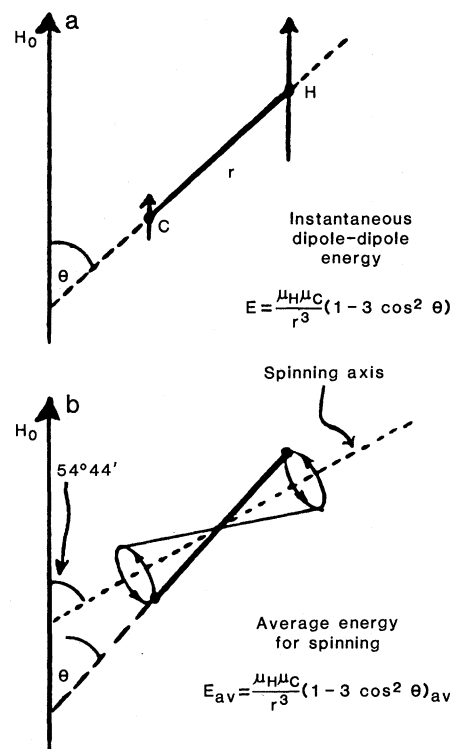


Fig. 2. Carbon-13-proton dipole-dipole interaction. (a) Static  $^{13}\text{C}$ - $^1\text{H}$  pair. (b) Effect of magic-angle spinning.

precisely defined pulses and rapid probe response, and has proved to be a difficult experiment to implement in several laboratories. This approach has until recently not shown a high enough level of resolution to promise a major impact on applications. As a consequence, it has never assumed the stature of a routine method that is widely used in chemical applications. However, multiple-pulse homonuclear  $^1\text{H}$  decoupling techniques are now showing considerable promise for expanding the horizons of  $^{13}\text{C}$  NMR experiments (as discussed below). In addition, recent experiments in which  $^1\text{H}$  spectra have been obtained by a combination of  $^1\text{H}$  multiple-pulse homonuclear decoupling and MAS have shown considerable promise (8).

Many of the nuclides that are of potential NMR interest for solids (especially for studies of heterogeneous catalysts) have values of the spin quantum number ( $I$ ) greater than  $1/2$ . For such nuclides, a third line-broadening effect that can be dominant must be addressed, the nuclear electric quadrupole interaction (9). This interaction is a manifestation of the fact that for nuclei with  $I \geq 1$  the nuclear electric charge distribution is not spherically symmetric; hence, the nuclear spin energy depends on the orientation of the nuclear spin relative to its local molecular electronic environment, as well as its orientation relative to  $H_0$ . The perturbations of the Zeeman energy levels brought about by this interaction are shown to first order in perturbation theory in Fig. 4 for the case of  $I = 5/2$ , to which  $^{27}\text{Al}$  belongs. The features shown

in Fig. 4 are representative for  $I$  is  $n/2$ , where  $n$  is an odd integer. For such cases, the frequency of the central transitions (Fig. 4c:  $-1/2 \leftrightarrow 1/2$ ) is unaffected to first order by the quadrupole interaction.

In contrast, the frequencies of the "outer" transitions (for instance,  $1/2 \leftrightarrow 3/2$ ) are affected to an extent that depends on the size of the nuclear electric quadrupole moment (a nuclear property), on the local electric field gradient generated at the nucleus by the molecular electrical environment, and on the orientation of the electric field gradient elements with respect to  $H_0$ . As the last of these varies randomly for an amorphous solid or a powdered sample, a quadrupolar powder pattern is the result for the "outer" lines. For most solid samples of chemical interest this line-broadening effect is so large that the outer lines are broadened beyond the detection limits of many spectrometers. For similar reasons, since there is no central ( $-1/2 \leftrightarrow 1/2$ ) transition for nuclides with integral values of  $I$ , the powder patterns for such nuclides are typically too broad to yield high-resolution NMR information.

As a consequence of these considerations, high-resolution NMR experiments on solids with quadrupolar nuclides are generally limited to the central transitions of nuclei with odd half-integer spins (10, 11). Rapid sample spinning is typically useful for such studies. Although MAS is useful in averaging the CSA and some dipole-dipole interactions for these kinds of experiments, there is a

second-order quadrupolar effect for the central transition, and this is not averaged to zero by MAS. The importance of the second-order quadrupole interaction decreases as  $H_0$  is increased, so second-order quadrupolar powder patterns and the associated complex pattern of sidebands produced by spinning modulation can be reduced dramatically at higher fields (11). This is perhaps the most important high-field advantage in solid-state NMR, and one can expect dramatic improvements for such nuclei as  $^{27}\text{Al}$  as increasingly intense fields become available.

Figure 5 shows  $^{27}\text{Al}$  NMR spectra of static and MAS experiments of  $\gamma$ -alumina at two fields, illustrating the spectral simplification at higher field. Appreciably sharper  $^{27}\text{Al}$  lines can usually be obtained for a zeolite sample, reflecting the more highly ordered structure of this kind of aluminosilicate system and attenuation of  $^{27}\text{Al}$ - $^{27}\text{Al}$  interactions (11).

The interactions described above constitute the main line-broadening influences in diamagnetic solids and can be averaged to zero by dissolving the sample in a liquid or by employing one of the recently developed line-narrowing techniques with the solid sample. For paramagnetic solids additional line-broadening influences exist because of dipolar and/or contact interactions between unpaired electron spins and the nuclear spins one wishes to detect (2). As the magnetic moment of an unpaired electron is three orders of magnitude larger than that of any nucleus, one might expect powder patterns of immense width from this source. Indeed, the line-broadening effects of paramagnetic centers can be very large, but they are partially averaged by the usually rapid electron spin relaxation processes. In fact, the effects of unpaired electrons would largely be averaged away to a nondetectable effect were it not for the fact that the populations of the  $\alpha$  and  $\beta$  electron spin states are not equal. Hence, instead of averaging the effects of unpaired electron spins to zero, electron spin relaxation averages these effects to a population-weighted powder pattern, still a major line-broadening effect for nuclei that interact with unpaired spins. The effect of dissolving such a system in a liquid solvent, or very rapid MAS, would be to average further the population-weighted average described above, resulting in sharpened signals that display what are known as contact or pseudocontact shifts. To date, relatively little has been reported on the application to paramagnetic samples of high-resolution NMR techniques for solids (12).

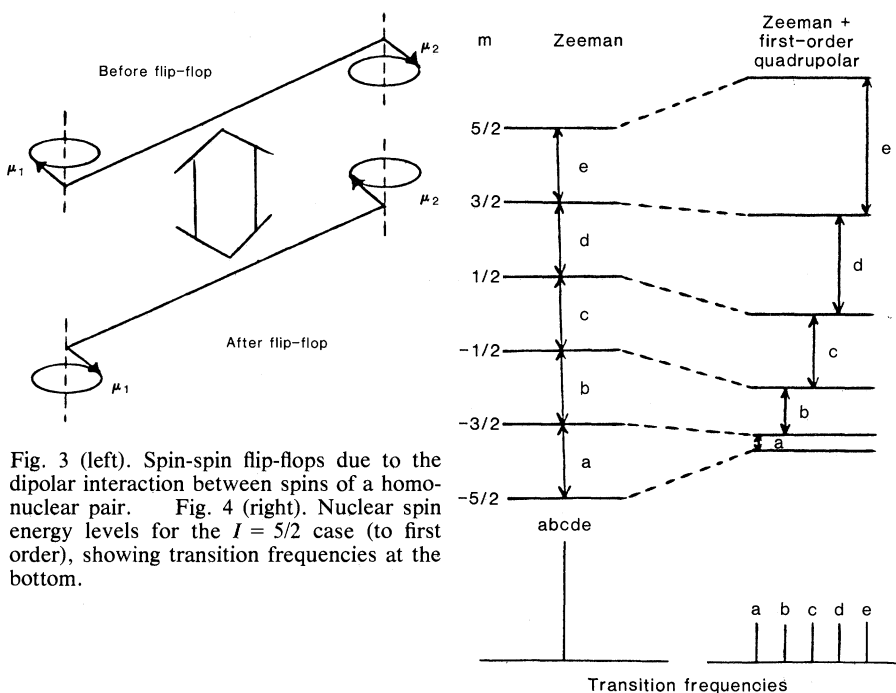


Fig. 3 (left). Spin-spin flip-flops due to the dipolar interaction between spins of a homonuclear pair. Fig. 4 (right). Nuclear spin energy levels for the  $I = 5/2$  case (to first order), showing transition frequencies at the bottom.

## Generating Magnetization for NMR in Solids

Another issue that often must be addressed for NMR observation in the solid state, especially for spin-1/2 nuclides, is how quickly the nuclear magnetization can be regenerated for rapid experiment repetition to build up the signal-to-noise ratio of the observed spectra. As spin-lattice relaxation is in many cases inefficient in solids, the common (pulse-observe-delay)<sub>n</sub> sequence used for liquid samples is often impractical, or at least very inefficient. Nevertheless, there is sometimes no reasonable alternative. Fortunately, for many common types of samples, including <sup>13</sup>C spectra of most organic solids, another approach is available for generating the magnetization to be observed in a solid-sample NMR experiment.

In their demonstration of the utility of high-power <sup>1</sup>H decoupling in solid-state <sup>13</sup>C NMR, Pines *et al.* (6) introduced the use of cross polarization (CP) for circumventing the time bottleneck of inefficient <sup>13</sup>C spin-lattice relaxation. In the CP approach <sup>1</sup>H spin polarization is transferred to <sup>13</sup>C polarization on a millisecond time scale. This is done by generating a state of low <sup>1</sup>H spin temperature with the <sup>1</sup>H magnetization colinear with a proton radio frequency (RF) field ( $H_{1H}$ ) and then placing the <sup>13</sup>C spin set in efficient thermal contact with the <sup>1</sup>H spin set by applying a <sup>13</sup>C RF field ( $H_{1C}$ ) under the Hartmann-Hahn condition (13),  $\gamma_H H_{1H} = \gamma_C H_{1C}$  where the  $\gamma$ 's represent nuclear magnetogyric ratios. Under this condition, as shown schematically in Fig. 6, there is a strong static component of the relationship between the precessional motions of individual <sup>1</sup>H and <sup>13</sup>C magnetic moments about their respective RF fields. The Hartmann-Hahn condition provides for efficient transfer of energy and spin polarization between the two spin manifolds, bringing about a decrease in the <sup>13</sup>C spin temperature and consequent generation of <sup>13</sup>C magnetization along  $H_{1C}$ . It is the decay behavior of the <sup>13</sup>C magnetization thereby generated that is repeatedly stored in a computer memory for Fourier transformation to provide the <sup>13</sup>C spectrum.

One of the key features of the generation of cross polarization from an *I* spin set (for example, <sup>1</sup>H) to an *S* spin set (<sup>13</sup>C) is that it relies on a strong, static component of *I-S* dipolar interaction. Hence, it is not very effective for liquid-like, mobile species, but is efficient for static or immobile species. This is in contrast to the "usual" spin-lattice relaxation ap-

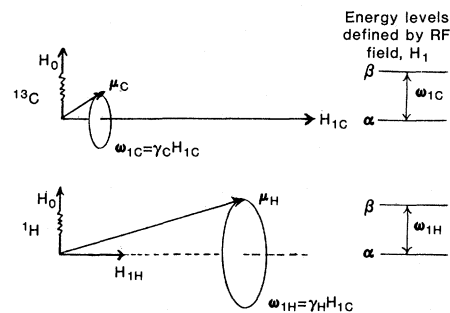
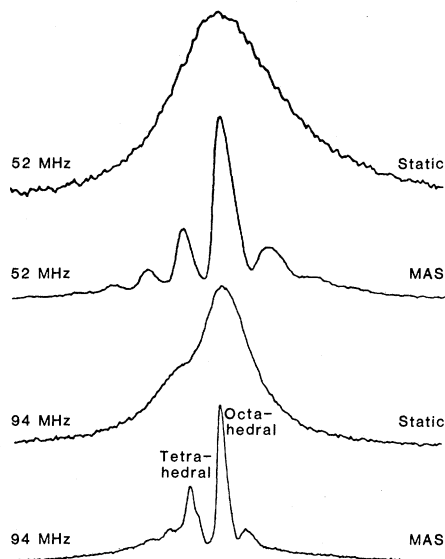


Fig. 5 (left). Aluminum-27 NMR spectra of  $\gamma$ -alumina at two fields, with and without MAS. (Note assignments of tetrahedral and octahedral sites in bottom spectrum.) Fig. 6 (right). Mechanism of cross polarization, showing precession of <sup>13</sup>C and <sup>1</sup>H nuclear magnetic moments about RF fields. Hartmann-Hahn match corresponds to  $\omega_{1H} = \omega_{1C}$ .

proach for generating magnetization, a method that relies on motional frequency components in the range of the Larmor frequency and hence is most effective for mobile species—that is, liquids. These kinds of differences between CP and spin-lattice relaxation behavior can be used to distinguish between mobile and immobile components of an inhomogeneous system. Furthermore, the dependence of CP efficiency on the strength of the *I-S* dipolar interaction can be used to discriminate against resonances of *S* nuclei that are far removed from the nearest *I* nuclei (14). For example, if protons ( $I = ^1\text{H}$ ) are located only at the surface of a system (such as OH groups on silica or organometallic moieties attached to a substrate), then *I-S* cross polarization provides a surface-selective approach for *S*-spin observation (15).

For paramagnetic solid samples an alternative means of generating nuclear spin magnetization for NMR observation can be used. This is dynamic nuclear polarization (DNP), a method by which nuclear spin magnetization is generated through the interactions between unpaired electron spins and nuclear spins (16). Dynamic nuclear polarization has long been an attractive approach, in principle, for the study of solids that contain paramagnetic centers, and recently the Delft University group convincingly demonstrated this potential (16, 17). In the DNP experiment transitions between electron spin resonance (ESR) energy levels are stimulated by microwave radiation at or near the ESR frequency, causing a major change in the populations of electron spin states. Because of the interaction between electron spins and nuclear spins, this perturbation in the ESR system manifests itself in the

nuclear spin system of a solid sample as a polarization (of nuclear spin state populations) by one or more of the following three mechanisms: the Overhauser effect, the solid-state effect, and the thermal mixing effect. There are at least two major effects that the DNP experiment has on the observation of nuclear spins. First, because of an electron spin "decoupling effect" it is often possible to observe an NMR signal of a paramagnetic sample that would otherwise not be observable because of severe broadening. Second, under appropriate conditions, DNP can result in a very large sensitivity enhancement in the NMR signal detected, the exact extent of the enhancement depending on a complex interplay of dynamical factors. The Delft group has incorporated MAS into the DNP <sup>13</sup>C experiment, with and without cross polarization (16). Large DNP enhancement factors have been obtained, and significant information has been obtained regarding the distribution of free radicals in coal. Although the use of spin labels in DNP work has not yet been exploited, it appears that there is substantial potential for this approach in a variety of problems in solid-state science.

## Popular Solid-Sample NMR Approaches

By far the most popular high-resolution NMR technique for solids, and the one that has had the most success in applications, has been the <sup>13</sup>C experiment employing a combination of cross polarization and magic-angle spinning (5, 18, 19). In 1976 Schaefer and Stejskal (19) introduced the <sup>13</sup>C CP-MAS experiment and demonstrated its routine appli-

capability to a variety of systems. Since that time, especially with the availability of commercial CP-MAS equipment, many laboratories have applied this approach to a wide range of problems, including natural and synthetic polymers (20, 21); solid organic geochemical samples such as coal (22), oil shale (23), humic acids, and fulvic acids (24); plant materials such as wood (25), seeds (26), and lignins (27); and surface systems (28); as well as fundamental chemical issues involving simple organic or organometallic systems (29). Indeed, the number of  $^{13}\text{C}$  CP-MAS applications is already so large that a comprehensive survey would be voluminous; hence, only representative references are given above.

The nature of the CP experiment lends itself to the measurement of an informative set of relaxation parameters, such as the  $^{13}\text{C}$  and  $^1\text{H}$  spin-lattice relaxation times (the latter measured via cross-polarized  $^{13}\text{C}$  magnetization),  $T_{1\rho}$  values for  $^1\text{H}$  and  $^{13}\text{C}$ , and the time constant ( $T_{\text{CH}}$ ) characterizing the cross-polarization process itself. Measurement of such relaxation parameters can provide valuable information on time-dependent phenomena (such as motions) in solids and has been especially useful for the study of dynamics in synthetic polymers (21).

A wide variety of spectral characteristics are obtained by the CP-MAS approach for  $^{13}\text{C}$  and other nuclides that have been observed by this method (for instance,  $^{15}\text{N}$ ,  $^{29}\text{Si}$ ,  $^{31}\text{P}$ ,  $^{113}\text{Cd}$ ). For  $^{13}\text{C}$  the spectra range from the collection of sharp lines that one expects for powdered samples of pure crystalline solids to the two broadbands characteristic of the spectra of coals, with the line widths of a typical synthetic polymer spectrum being intermediate, as shown in Fig. 7. The main reason for the larger line width of the polymer spectra, compared to pure crystalline powders, is the distribution of conformations typical in a synthetic polymer, each slightly different conformation having its own characteristic set of  $^{13}\text{C}$  chemical shifts. For samples that are extremely complex mixtures, such as coal, it is primarily the distribution of isotropic chemical shifts of similar, but slightly different, chemical structures that gives rise to the typically broadbands (one band for  $sp^3$  carbons and one for  $sp^2$  carbons).

One of the important issues that it has been necessary to face as MAS experiments have become increasingly popular is the spinning sidebands that arise because of the periodic modulation of the chemical shift by sample spinning (30). This problem becomes increasingly seri-

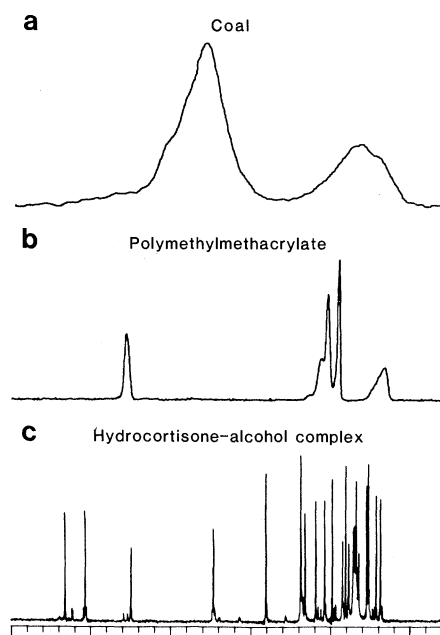


Fig. 7. Representative  $^{13}\text{C}$  CP-MAS spectrum for (a) coal, (b) a synthetic polymer, and (c) a pure crystalline organic.

ous as the static magnetic field strength is increased. Therefore, the popularity of higher field spectrometers has generated interest in developing approaches for suppressing or avoiding the spinning sidebands. Although some elegant methods have been advanced (31, 32), until the performance characteristics of these methods have been more firmly established, many laboratories have chosen lower field spectrometers for work on systems with large chemical shift anisotropies (such as aromatic and carbonyl carbons).

The "standard" CP-MAS approach outlined above, in which one relies on the separation of signals due to the dispersion of isotropic chemical shifts to distinguish different chemical structural environments, might be considered the first generation in modern high-resolution NMR experiments for solids. What one might consider second-generation CP-MAS approaches are characterized by making use of the time domain to distinguish between otherwise overlapping resonances that correspond to distinct structural situations. According to this strategy one looks for differences in the incoherent evolution of magnetization—relaxation phenomena—in order to make structural distinctions. Perhaps the most popular and useful of this class of techniques is the interrupted-decoupling or dipolar-dephasing experiment (33). In this experiment, as applied to  $^{13}\text{C}$ , the magnetization of  $^{13}\text{C}$  nuclei to which one or more protons are directly bonded is allowed to evolve (dephase)

during a period in which the decoupler is off. This evolution is essentially incoherent because of the time dependences imparted by spinning and, more important,  $^1\text{H}$ - $^1\text{H}$  spin-spin flip-flops (5). With typically 40 to 100  $\mu\text{sec}$  of decoupling interruption, magnetization of only carbons without directly attached protons (or with very mobile C-H vectors, as in rapidly rotating  $\text{CH}_3$  groups) survive strongly in the  $^{13}\text{C}$  CP-MAS spectrum. Several laboratories have explored the use of this and other second-generation techniques for extracting structural information from complex  $^{13}\text{C}$  (and  $^{15}\text{N}$ ) CP-MAS spectra.

The need for "crisper" structural distinctions than are usually provided by first-generation or second-generation approaches for complex systems with overlapping chemical shifts (such as coal) has maintained interest in the development of additional capabilities. A  $^{13}\text{C}$  experiment in which, in order to distinguish one structural environment from another, one takes advantage of the coherent time development due to the specific interaction of a given  $^{13}\text{C}$  nucleus with another nucleus or group of nuclei in its specific structural environment might be considered a third-generation approach. Considerable effort in several laboratories has been directed to the development of this class of approaches. However, whenever one is relying on the interaction between a specific carbon and one or more specific protons (not an average interaction between carbons and hydrogens) to distinguish the carbon environment, the goal of the experiment is usually undermined substantially by the "scrambling" of proton spins due to the rapid  $^1\text{H}$ - $^1\text{H}$  spin flip-flops that are characteristic of most organic solids. For example, it is necessary to eliminate rapid  $^1\text{H}$ - $^1\text{H}$  flip-flops in order to obtain  $^1\text{H}$  spectral information in a solid-sample two-dimensional Fourier transform heteronuclear chemical shift correlation experiment with  $^{13}\text{C}$  detection (34). Homonuclear  $^1\text{H}$  decoupling techniques are available for overcoming the strong  $^1\text{H}$ - $^1\text{H}$  dipolar interactions responsible for these often debilitating  $^1\text{H}$ - $^1\text{H}$  flip-flops (7) and are being implemented in several laboratories.

Probably the most successful applications for homonuclear decoupling of  $^1\text{H}$ - $^1\text{H}$  interactions in  $^{13}\text{C}$  CP-MAS experiments to date have been in the observation of scalar C-H couplings (35, 36). Recently reported variants of this experiment, in which the evolution of  $^{13}\text{C}$  magnetization under the influence of  $J_{\text{CH}}$  (with  $^1\text{H}$ - $^1\text{H}$  flip-flops suppressed by  $^1\text{H}$  multiple-pulse techniques) is used to dis-

tinguish among  $\equiv\text{C}-$ ,  $\equiv\text{CH}$ ,  $=\text{CH}_2$ , and  $-\text{CH}_3$  groups (36), are direct solid-state analogs of the "spectral editing" techniques that have become so popular in liquid-sample  $^{13}\text{C}$  NMR. Direct observation of  $J_{\text{CH}}$  splittings in pure organic solids will be of considerable fundamental importance, but will have little applicability to typical complex organic solids. However, the ability to detect selectively  $\equiv\text{C}-$ ,  $\equiv\text{CH}$ ,  $=\text{CH}_2$ , or  $-\text{CH}_3$  on the basis of evolution under  $J_{\text{CH}}$  should have important consequences in many applications.

### Recent Advances

A development that may represent one of the most significant new approaches in NMR in several years is zero-field NMR. This approach, developed by the Pines group (37), derives its name from the fact that the characteristics of the zero-field NMR spectrum are determined during an incrementally varied evolution period ( $t_1$ ) in which the sample experiences no external magnetic field. A mechanical device is employed to move the sample from a position inside the field of a superconducting solenoid to a position outside it, so that a strong applied magnetic field can be used before and after the  $t_1$  period to generate and observe, respectively, the magnetization that evolves during  $t_1$ . Fourier transformation of the observed NMR signal with respect to the variable  $t_1$  yields a NMR spectrum that is characteristic of the interactions present during the zero-field  $t_1$ . In this sense, the strategy is analogous to that of obtaining information on interactions present during the evolution period of a "standard" two-dimensional Fourier transform NMR experiment (38).

However, in the zero-field case, there is no  $H_0$  present during the evolution period, so there is no directional character to the interaction due to the orientation of the sample in the sense described for the chemical shift, dipole-dipole interaction, and nuclear electric quadrupole interaction (for instance, see Figs. 1, 2, and 4). Hence, even when the sample is a powdered or amorphous solid, these interactions do not give rise to powder patterns, since the orientation dependence on which the powder pattern is based is absent. The net result is that the zero-field spectrum has the kind of sharp peaks one might expect of the spectra of single crystals, with splittings that contain valuable structural information, for example, internuclear distances from dipolar splittings.

Although the interpretation of zero-field NMR spectra of complex systems can be very complicated, rapid progress is being made. Considerable promise has already been demonstrated for the elucidation of dipolar and quadrupolar interactions in powdered samples.

Other recently developed techniques for high-resolution NMR in solids include alternatives to MAS and dilute-spin (for example,  $^{13}\text{C}$ ) NMR imaging of solids. Two-dimensional experiments have been developed for the determination of individual powder patterns corresponding to each isotropic chemical shift in the spectrum. These techniques each involve one of two mechanical alternatives to the usual MAS method. One employs discrete  $120^\circ$  "hops" of the sample about the magic-angle axis (39), and the other utilizes rapid "flipping" of the sample spinning axis between the magic-angle orientation and some other orientation (40).

In order to circumvent the dominating influences of  $^1\text{H}-^1\text{H}$  dipolar interactions in  $^1\text{H}$  NMR imaging experiments on solids, a  $^{13}\text{C}$  CP technique has been developed for NMR imaging of simple solids (41). For cases in which the  $^{13}\text{C}$  CSA's are small, this technique provides chemical shift-selective images, and it seems likely that the limitation to small CSA's can be removed by employing a variation of the sample hopping technique mentioned above.

### Conclusions

The dramatic development of solid-sample NMR techniques of the past few years has thrust high-resolution NMR into the realm of solid-state science. The rapid evolution of this field includes the continuing emergence of important new techniques, and shows promise of making NMR as valuable for the characterization of solid samples as it has been for the study of liquids.

### References and Notes

- R. K. Harris, *Nuclear Magnetic Resonance* (Pittman, London, 1983); J. A. Pople, W. G. Schneider, H. J. Bernstein, *High-Resolution Nuclear Magnetic Resonance* (McGraw-Hill, New York, 1959); T. C. Farrar and E. D. Becker, *Pulse and Fourier Transform NMR* (Academic Press, New York, 1971).
- G. E. Maciel, in *Magnetic Resonance. Introduction, Advanced Topics and Applications to Fossil Energy*, L. Petrakis and J. P. Fraissard, Eds. (NATO ASI Series, Reidel, Boston, 1984).
- M. Mehring, *High Resolution NMR Spectroscopy in Solids* (Springer-Verlag, New York, ed. 2, 1983); U. Haeberlen, *High Resolution NMR in Solids. Selective Averaging* (Academic Press, New York, 1976).
- E. R. Andrew, *Prog. NMR Spectrosc.* **8**, 1 (1971); I. J. Lowe, *Phys. Rev. Lett.* **2**, 285 (1959); H. Kesslemeier and R. E. Norberg, *Phys. Rev.* **155**, 321 (1967).
- C. S. Yannoni, *Acc. Chem. Res.* **15**, 201 (1982).
- A. Pines, M. G. Gibby, J. S. Waugh, *J. Chem. Phys.* **59**, 569 (1973).
- J. S. Waugh, L. M. Huber, U. Haeberlen, *Phys. Rev. Lett.* **20**, 180 (1968); P. Mansfield, M. J. Orchard, D. C. Stalker, K. H. B. Richards, *Phys. Rev. B* **7**, 90 (1973); W. K. Rhim, D. D. Ellemann, R. W. Vaughan, *J. Chem. Phys.* **59**, 3740 (1973); W. K. Rhim, D. D. Ellemann, L. B. Schreiber, R. W. Vaughan, *ibid.* **60**, 4595 (1974); D. P. Burum and W. K. Rhim, *ibid.* **71**, 944 (1979); D. P. Burum, M. Lindner, R. R. Ernst, *J. Magn. Reson.* **44**, 173 (1981).
- H. Rosenberger, *Z. Chem.* **23**, 34 (1983); \_\_\_\_\_ and G. Scheler, *ibid.* **22** (1982).
- A. Abragam, *The Principles of Nuclear Magnetism* (Oxford Univ. Press, London, 1961), chapter 7.
- D. Muller, W. Gessner, H.-I. Behrens, G. Scheller, *Chem. Phys. Lett.* **79**, 59 (1982).
- C. A. Fyfe, G. C. Gobbi, J. S. Hartmann, R. E. Lenkinski, J. H. O'Brien, E. R. Benge, M. R. Smith, *J. Magn. Reson.* **47**, 168 (1982); S. Schramm and E. Oldfield, *J. Am. Chem. Soc.* **106**, 2502 (1984); M. D. Meadows *et al.*, *Proc. Natl. Acad. Sci. U.S.A.* **79**, 1351 (1982); S. Schramm, R. Kirkpatrick, E. Oldfield, *J. Am. Chem. Soc.* **105**, 2483 (1983).
- V. P. Chacko, S. Ganapathy, R. G. Bryant, *J. Am. Chem. Soc.* **105**, 5491 (1983).
- S. R. Hartmann and E. L. Hahn, *Phys. Rev.* **128**, 2042 (1962).
- L. B. Alemany, D. M. Grant, R. J. Pugmire, T. J. Alger, K. Zilm, *J. Am. Chem. Soc.* **105**, 2133 (1983); *ibid.*, p. 2142.
- G. E. Maciel and D. W. Sindorf, *ibid.* **102**, 7606 (1980); D. W. Sindorf and G. E. Maciel, *ibid.* **105**, 1487 (1983); *J. Phys. Chem.* **87**, 5516 (1983).
- R. A. Wind *et al.*, *J. Magn. Reson.* **52**, 424 (1983); R. A. Wind, M. J. Duijvestijn, C. V. D. Lugt, J. Smidt, J. Vriend, in *Magnetic Resonance. Introduction, Advanced Topics and Applications to Fossil Energy*, L. Petrakis and J. P. Fraissard, Eds. (NATO ASI Series, Reidel, Boston, 1984).
- R. A. Wind, J. Trommel, J. Smidt, *Fuel* **58**, 900 (1979); *ibid.* **61**, 398 (1982).
- J. Schaefer and E. O. Stejskal, in *Topics in Carbon-13 NMR Spectroscopy*, G. C. Levy, Ed. (Wiley-Interscience, New York, 1979); R. E. Wasylshen and C. A. Fyfe, *Annu. Rep. NMR Spectrosc.* **12**, 1 (1982); G. E. Maciel and M. J. Sullivan, *ACS Monogr.* **191** (1982), p. 319.
- J. Schaefer and E. O. Stejskal, *J. Am. Chem. Soc.* **98**, 1031 (1976).
- G. E. Maciel, I.-S. Chuang, L. Gollob, *Macromolecules* **17**, 1081 (1984); G. E. Maciel, N. M. Szeverenyi, T. E. Early, G. E. Myers, *ibid.* **16**, 598 (1983).
- J. Schaefer, E. O. Stejskal, R. Buchdahl, *ibid.* **10**, 284 (1977); *ibid.* **8**, 291 (1975); T. R. Steger, J. Schaefer, E. O. Stejskal, R. A. McKay, *ibid.* **13**, 1127 (1980); M. D. Sefcik, J. Schaefer, E. O. Stejskal, R. A. McKay, *ibid.*, p. 1132; J. Schaefer, M. D. Sefcik, E. O. Stejskal, R. A. McKay, *ibid.* **14**, 188 (1981); W. L. Earl and D. L. VanderHart, *ibid.* **12**, 762 (1979); D. L. VanderHart and A. N. Garroway, *J. Chem. Phys.* **71**, 2773 (1979); *ibid.*, p. 1773; A. N. Garroway, W. B. Moniz, H. A. Resing, *Faraday Symp. Chem. Soc.* (1979), p. 63.
- G. E. Maciel, V. J. Bartuska, F. P. Miknis, *Fuel* **58**, 391 (1979); G. E. Maciel, M. J. Sullivan, N. Szeverenyi, F. P. Miknis, *AIP Conf. Proc. No. 70* (1981), pp. 66-81; M. J. Sullivan and G. E. Maciel, *Anal. Chem.* **54**, 1615 (1982); *ibid.*, p. 1606.
- H. A. Resing, A. N. Garroway, R. N. Hazlett, *Fuel* **57**, 450 (1978); A. R. Palmer and G. E. Maciel, *Anal. Chem.* **54**, 2194 (1982); F. P. Miknis, N. M. Szeverenyi, G. E. Maciel, *Fuel* **61**, 341 (1982).
- P. G. Hatcher, I. A. Breger, L. W. Dennis, G. E. Maciel, *Terrestrial and Aquatic Humic Materials*, R. F. Christman and O. Giessing, Eds. (Ann Arbor Press, Ann Arbor, Mich., 1983), p. 37.
- W. Kolodziejewski, J. S. Frye, G. E. Maciel, *Anal. Chem.* **54**, 1419 (1982); J. F. Haw, G. E. Maciel, H. A. Schroeder, *ibid.* **56**, 1323 (1984).
- D. J. O'Donnell, J. J. H. Ackerman, G. E. Maciel, *J. Agric. Food. Chem.* **29**, 514 (1981); J. F. Haw and G. E. Maciel, *Anal. Chem.* **55**, 1262 (1982).
- V. J. Bartuska, G. E. Maciel, H. I. Bolker, B. I. Fleming, *Holzforchung* **34**, 214 (1980); G. E. Maciel, V. J. Bartuska, J. J. H. Ackerman, D. J. O'Donnell, B. L. Hawkins, *Makromol. Chem.* **182**, 2297 (1981).
- J. F. Haw, I.-S. Chuang, B. L. Hawkins, G. E. Maciel, *J. Am. Chem. Soc.* **105**, 7206 (1983); G. E. Maciel *et al.*, *ibid.*, p. 5529; W. P. Rothwell, W. X. Shen, J. H. Lunsford, *ibid.* **106**, 2452 (1984); W. H. Dawson, S. W. Kaiser, P. D.

- Ellis, R. R. Inners, *J. Phys. Chem.* **86**, 867 (1982).
29. C. S. Yannoni, V. Macho, P. C. Myhre, *J. Am. Chem. Soc.* **104**, 907 (1982); *ibid.*, p. 7380; N. M. Szeverenyi, A. Bax, G. E. Maciel, *ibid.* **105**, 2579 (1983).
30. M. M. Maricq and J. S. Waugh, *Chem. Phys. Lett.* **47**, 327 (1977); *J. Chem. Phys.* **70**, 3300 (1979).
31. W. T. Dixon, *J. Magn. Reson.* **44**, 220 (1981); ———, J. Schaefer, M. D. Sefcik, E. O. Stejskal, R. A. McKay, *ibid.* **45**, 173 (1981); W. T. Dixon, J. Schaefer, M. D. Sefcik, E. O. Stejskal, R. A. McKay, *ibid.* **49**, 341 (1982); W. T. Dixon, *J. Chem. Phys.* **77**, 1800 (1982).
32. W. P. Aue, D. J. Ruben, R. G. Griffin, *J. Chem. Phys.* **80**, 1729 (1984).
33. S. J. Opella and M. H. Frey, *J. Am. Chem. Soc.* **101**, 5854 (1979); L. B. Alemany, D. M. Grant, T. G. Alger, R. J. Pugmire, *ibid.* **105**, 6697 (1983).
34. P. Caravatti, G. Bodenhausen, R. R. Ernst, *Chem. Phys. Lett.* **89**, 363 (1983); J. E. Roberts, S. Vega, R. G. Griffin, *J. Am. Chem. Soc.* **106**, 2506 (1984).
35. K. W. Zilm and D. M. Grant, *J. Magn. Reson.* **48**, 524 (1982); T. Terao, H. Miura, A. Saika, *J. Chem. Phys.* **75**, 1573 (1981).
36. L. Mayne, R. J. Pugmire, D. M. Grant, *J. Magn. Reson.* **56**, 151 (1984); T. Terao, H. Miura, A. Saika, *J. Am. Chem. Soc.* **104**, 529 (1982).
37. T. H. Maugh II, *Science* **224**, 793 (1984); D. P. Weitekamp, A. Bielecki, K. Zilm, A. Pines, *Phys. Rev. Lett.* **50**, 1807 (1983); A. Bielecki *et al.*, *J. Chem. Phys.* **80**, 2232 (1984).
38. A. Bax, *Two-Dimensional Nuclear Magnetic Resonance in Liquids* (Reidel, Boston, 1982).
39. A. Bax, N. M. Szeverenyi, G. E. Maciel, *J. Magn. Reson.* **52**, 147 (1983); N. M. Szeverenyi, A. Bax, G. E. Maciel, *ibid.*, in press.
40. A. Bax, N. M. Szeverenyi, G. E. Maciel, *ibid.* **55**, 494 (1983).
41. N. M. Szeverenyi and G. E. Maciel, *ibid.*, in press.

## Nuclear Magnetic Resonance Technology for Medical Studies

Thomas F. Budinger and Paul C. Lauterbur

Nuclear magnetic resonance (NMR) applications to medical science began nearly 30 years ago with proton NMR measurements on cells, excised frog muscles, arms of living humans, and the living rat (1). Based on the observations in 1971 that the proton NMR properties

adenosine triphosphate (ATP) and creatine phosphate as well as cellular pH have found clinical applications (4). More recently, use of  $^1\text{H}$  and  $^{13}\text{C}$  spectra to evaluate other compounds has shown equally important potentials for clinical studies (5).

**Summary.** Nuclear magnetic resonance proton imaging provides anatomical definition of normal and abnormal tissues with a contrast and detection sensitivity superior to those of x-ray computed tomography in the human head and pelvis and parts of the cardiovascular and musculoskeletal systems. Recent improvements in technology should lead to advances in diagnostic imaging of the breast and regions of the abdomen. Selected-region nuclear magnetic resonance spectroscopy of protons, carbon-13, and phosphorus-31 has developed into a basic science tool for in vivo studies on man and a unique tool for clinical diagnoses of metabolic disorders. At present, nuclear magnetic resonance is considered safe if access to the magnet environment is controlled. Technological advances employing field strengths over 2 teslas will require biophysical studies of heating and static field effects.

of normal and malignant rat tissues differ (2) and in 1972 that NMR can be used to form images (3), technological and commercial activities of increasing intensity have focused on proton NMR imaging of the human body. At present, NMR imaging provides an anatomical description of soft tissues with a better contrast resolution than x-ray computed tomography (CT) in most areas of the body. Following the discovery of the relation between the phosphorus NMR spectra and the metabolites of red blood cells, in vivo evaluations of the concentration of high-energy phosphate compounds such as

This article is a report on the status of nuclear magnetic resonance imaging from theoretical and clinical viewpoints as expressed at a National Academy of Sciences symposium held in late 1983 (6), with a review of additional relevant information on in vivo spectroscopy reported in the literature through early 1984. A description of NMR theory and relaxation parameters relevant to NMR imaging is followed by an analysis of modern imaging strategies, signal-to-noise ratio, contrast agents, in vivo spectroscopy, spectroscopic imaging, clinical applications, and safety.

The theory of NMR is reviewed in a number of recent sources (7). Most elements have at least one reasonably abundant isotope whose nucleus is magnetic. The magnetic nuclei or nuclear spins of high abundance in biological material are  $^1\text{H}$ ,  $^{13}\text{C}$ ,  $^{23}\text{Na}$ ,  $^{31}\text{P}$ , and  $^{39}\text{K}$ . In an external magnetic field these nuclear spins behave like small magnets and assume a low-energy state aligned with the field or a higher energy state aligned against the field. The hydrogen nucleus (proton) is abundant in the body because of the high water content of nonbony tissues. When the body is immersed in a static magnetic field, slightly more protons become aligned with the magnetic field than against the static field. At 0.25 T (2500 gauss) and 25°C the difference between these aligned populations of about one proton in a million produces a net magnetization. A rapidly alternating magnetic field at an appropriate radio frequency (RF), applied by a coil near the subject or specimen in the static magnetic field, changes the orientation of the nuclear spins relative to the direction of the strong static magnetic field (Fig. 1). The changes are accompanied by absorption of energy by protons which undergo the transition from a lower energy state to the higher energy state. When the alternating field is turned off, the nuclei return to the equilibrium state with the emission of energy at the same frequency as that of the stimulating alternating field (RF). That frequency is the resonance or Larmor frequency, given by  $\nu = (\gamma/2\pi)B$ , where  $\gamma$  is the characteristic gyromagnetic ratio of the nucleus and  $B$  is the static magnetic field. The nuclei of different elements, and even of different isotopes of the same element, have very different resonance frequencies.

Thomas F. Budinger is Henry Miller Professor at Donner Laboratory, Lawrence Berkeley Laboratory, and the Department of Electrical Engineering and Computer Sciences, University of California, Berkeley 94720, and the Department of Radiology, University of California, San Francisco 94122. Paul C. Lauterbur is University Professor, Professor of Chemistry, and Research Professor of Radiology, Department of Chemistry, State University of New York, Stony Brook 11794.